

Electrochemical Evaluation of Electrocatalysts for Fuel Cell Applications: A Practical Approach

Mohammed H. Atwan^{1,*}, Elod L. Gyenge², and Derek O. Northwood^{1,*}

¹General Motors R&D Technical Center (for Trison Engineering), Warren, MI 48090, USA

²Chemical and Biological Eng., The University of British Columbia, Vancouver, BC, V6T 1Z4, Canada

³Mechanical, Auto, and Materials Eng., University of Windsor, Windsor, N9B 3P4, Canada

Received: July 29, 2009, Accepted: August 4, 2009

Abstract: The application of various electrochemical techniques to evaluate the activity of supported nano-size electrocatalysts for the oxidation of a specific fuel for fuel cell applications is examined. Cyclic voltammetry (CV) on both static and dynamic (rotating disc electrode, RDE) electrodes, and fuel cell station tests were the main electrochemical techniques used in this study. It was found from both static and dynamic CV and the fuel cell station tests that the most active catalyst is the one that shows the most negative oxidation peak potential. According to the Tafel equation, a lower anodic/cathodic overpotential is clear evidence of higher catalytic activity. This can be achieved for a specific current load by an electrocatalyst that exhibits as low a Tafel slope, and as high an exchange current density, as possible. RDE and fuel cell station tests show that the best performance was recorded for those electrocatalysts which have values of the Tafel slope (ba) and the exchange current density (io) that, on balance, give rise to the lowest overpotential. Therefore, CV and RDE are the recommended electrochemical techniques for a reliable assessment of electrocatalysts prior to performing a “real” fuel cell test.

Keywords: electrocatalysts, fuel cells, electrochemical.

1. INTRODUCTION

1.1. Techniques for Study of Electrode Kinetics

A large number of electrochemical techniques are available to study the electrode processes for both electrosynthesis and galvanic cell applications [1, 2]. Potential, current, concentration, and time are the fundamental parameters measured using electrochemical techniques. The relationship among these parameters is quite complex and depends on: which of these parameters is kept constant; the type of mass transfer mode; the kinetics of both the electrochemical and the chemical reactions that accompany the electron-transfer reaction; and the geometry of both the working electrode and the cell [3].

A quick electrode reaction screening can be made by applying controlled-potential or controlled-current techniques on either static or dynamic electrodes. Information on the reaction rate, the reaction mechanism(s), intermediates, and the adsorption process can be obtained from the resulting controlled-potential or controlled-current data [2]. For a better and more accurate study of

the adsorption processes, Bard and Mirkin [4] have suggested that it is better not to rely on purely electrochemical methods, but rather use a combination of electrochemical and spectroscopic techniques [4].

Combinatorial methods have been applied as a rapid-throughput method to evaluate potential catalysts for a specific reaction, using multi-potentiostats [5-7]. Individually controllable electrodes are utilized in this method, and each electrode is essentially a miniature fuel cell. The main advantage of this method is to save time in screening a number of electrodes at once. Combinatorial methods and spectroscopic techniques utilize basic electrochemical techniques, mainly cyclic voltammetry on both static and dynamic electrodes, in order to calculate the Tafel and other electrochemical parameters [4-7].

1.2. Electrocatalysts

Electrocatalysts, like catalysts for ‘conventional’ reactions, provide an alternative path that lowers the activation energy of the reaction. Hence, electrode reactions can occur at higher exchange current densities. The energy efficiency of any cell is greatly af-

*To whom correspondence should be addressed: Email: dnorthwo@uwindsor.ca and mohammed.atwan@gm.com

ected by overpotentials at both the anode and the cathode that result from the required or applied current/potential. According to the Tafel equation, the required overpotential depends on both the exchange current density and the Tafel slope [8, 9]. A low overpotential indicates a high electrocatalytic activity, and this can be achieved, according to the Tafel equation, by lowering the Tafel slope and/or increasing the exchange current density. For surface reactions, such as in electrocatalytic processes, the rate determining step is the surface reaction. Therefore, the measured current density depends on both the intrinsic electrocatalytic activity of the catalyst's surface and its real surface area. Accordingly, changing the surface electronic properties by supporting the metal catalyst on a conductive substrate(s), or alloying with other element(s), can greatly enhance the value of the exchange current density [10].

It should also be noted that increasing the electrocatalyst surface area by supporting a nano-size electrocatalyst on a high surface area conductive substrate will enhance the catalytic activity and, therefore, a higher exchange current density will also be achieved [10].

Tafel slopes can vary with surface roughness. Porous electrodes differ significantly from planar electrodes [11]. It has been proposed that ionic conductivity, mass transfer limitations, the electrode kinetics, and the ohmic drop across the catalytic layer are among the reasons for the large apparent Tafel slopes of porous electrodes [12], in addition to the adsorption and intrinsic electrode kinetics effects [13].

1.3. Electrochemical Techniques for Study of Electrocatalysts

Heterogeneous reactions, e.g., electrocatalytic reactions, are complex. Therefore, their study requires the use of a number of electrochemical techniques [2,10]. It has been proposed that steady-state current measurement as a function of potential is the best electrochemical technique with which to start [10]. Additional information can be gained from cyclic voltammetry (CV) on both static and dynamic electrodes, chronoamperometry (CA), chronopotentiometry (CP), and capacitance measurements [10]. A detailed insight into the electrode-solution interface during the electrocatalytic reaction can also be obtained by *in situ* and *ex situ* spectroscopic techniques [4].

The electrocatalytic activities of various fuels for fuel cell applications have been extensively investigated during the last four decades [14-44]. Most of the open literature publications used CV on both static and dynamics electrodes in their assessment of the catalytic activity of the various electrocatalysts towards the oxidation of the investigated fuels: see Table 1. None of these open literature publications has suggested a practical approach to identifying which of the electrochemical parameters have a significant effect on the fuel cell performance.

In this paper, we have taken a practical approach to demonstrate that electrochemical parameters such as peak potential, Tafel slope, and exchange current density obtained by CV on both static and dynamic electrodes have a significant effect on the fuel cell performance of an electrocatalyst. Hence, CV can be used as a reliable electrochemical technique to assess the electrochemical catalyst activity for a specific fuel prior to an actual fuel cell test.

2. EXPERIMENTAL METHODS

2.1. Colloidal Preparation Method

A range of colloidal metal catalysts (Pt, Pt-Au, Pt-Ni, Pt-Ir, Au, and Au-Pd) were prepared using a modified Bönnehan method [45] as described by Götz and Wendt [46]. The colloidal metals were prepared with a 20 %wt load on Vulcan XC72R support (L. V. LAMOS Limited). The alloying ratio was 1:1 atomic. A dry nitrogen glove box atmosphere was used to handle and weigh the reactants. The reactions were performed in a dry nitrogen atmosphere using Schlenk flasks and nitrogen lines.

Stoichiometric amounts of 1M of tetrabutylammonium chloride ($C_{16}H_{36}ClN$) in tetrahydrofuran (THF) (Sigma-Aldrich, >99% Anhydrous) and 1M of Lithium triethylhydroborate ($C_6H_{16}BLi$) in THF (Sigma-Aldrich, 1 M in THF, Anhydrous) were mixed to obtain a solution of 0.5M of tetrabutylammoniumtriethyl hydroborate, $N(C_{16}H_{36})_4[Be_3H]$. LiCl was removed by passing the reaction products solution through a D-4 glass frit. A 50% excess of 0.5M of tetrabutylammoniumtriethyl hydroborate, $N(C_{16}H_{36})_4[Be_3H]$, was added dropwise over a period of 1 h at 296 K to stirred suspensions of anhydrous metal salt(s) in 100 ml THF. Almost complete dissolution of the salt(s) (Sigma-Aldrich) occurred after stirring the deep dark coloured solution for 4 h. To destroy any unreacted reducing agent, 5 ml of acetone were added and stirred for 1 h. The solution then was added dropwise to a stirred suspension of the carbon support (Vulcan XC72R) in 100 ml THF. The mixture was stirred for 12 h. 150 ml of ethanol (Sigma-Aldrich, 99.5%, Anhydrous) were then added and stirred for 2 h. After filtering the reaction solution through a D-4 glass frit, the supported catalyst(s) was washed with ethanol several times, and then dried under a nitrogen vacuum at 296 K for 12 h.

Annealing and reducing processes were performed to remove the protective shell in order to enhance the catalytic activity [47-49]. The processes were performed in three stages using a controlled tubular furnace (LINDBERG). First, the samples were heated up to 300°C for 30 min under N_2 (5, BOC Gas) at a flow rate of 160 ml min^{-1} . In this stage most of the organic shell is decomposed. Second, the samples were annealed under a N_2/O_2 (5, BOC Gas) mixture (10 vol.% O_2) at a flow rate of 160 ml min^{-1} for 30 min at 300°C. Third, the samples were reduced under 100 vol.% H_2 at a flow rate of 160 ml min^{-1} for 30 min at 300°C, in order to reduce any oxidized metal(s) formed during the annealing processes. Nitrogen was purged for 5 min before and after the annealing process to avoid any contact between the oxygen and hydrogen gases.

2.2. Electrode and Cell Preparation for Electrochemical Methods

A glassy carbon disk electrode, 3 mm diameter, manufactured from a glassy carbon rod (Electrosynthesis Inc.), was used as a substrate for the colloids. Prior to each experiment, the glassy carbon (GC) electrode was polished to a mirror finish first with 1 mm diamond paste and then with 0.05 mm alumina (Cypress System Inc. polishing kit). The polishing was followed by a thorough washing and ultrasonic cleaning.

To create good bonding of the supported metal colloid catalysts to the GC electrode, 5 mg of the carbon supported catalyst powder (20 % wt metal) was dispersed ultrasonically for 45 minutes in a 1 ml solution composed of 0.25 ml of a Nafion solution 5 % wt (Aldrich) and 0.75 ml of ethanol (Aldrich). From the suspension of the supported catalyst and Nafion, 10 μ l was carefully applied on

Table 1. Summary of selected literature on the use of electrochemical techniques to evaluate the activity of electrocatalysts for fuel cell applications.

Researchers	Year	Fuel	Catalysts	Electrochemical Techniques		Reference No.
				Static	Dynamic	
M. Janssen, J. Moolhuysen	1976	Methanol	26 Pt-alloys	CV, LSV		14
B. McNicol, R. Short	1977	Methanol	PtRu/C	CV, LSV		15
A. Aramata, R. Ohnishi	1984	Methanol	Pt/Nafion	CV, CA		16
A. Aramata, et. al.	1988	Methanol	3 Pt-alloys	CC, CA		17
S. Swathirajan, et. al.	1991	Methanol	PtRu/C	LVS		18
A. Parthasarathy, et. al.	1991	O ₂ Reduction	Pt-Wire	CV, CA		19
F. Uribe, et. al.	1992	O ₂ Reduction	Pt/Nafion	CV		20
A. Parthasarathy, et. al.	1992	O ₂ Reduction	Pt/C	CV		21
S. Mukerjef, et. al.	1993	O ₂ Reduction	Pt/C	CV		22
L. Burke, et. al.	1994	Methanol	Pt/C	CV, LSV		23
P. Biswas, et. al.	1996	Methanol	Pt/C	CV		24
P. Kauranen, et. al.	1996	Methanol	Pt/C, PtRu/C	LSV		25
T. Schmidt, et. al.	1997	Hydrogen	PtRu Colloid	CV	CV on RDE	26
G. Lalande, et. al.	1997	O ₂ Reduction	Fe-Based	CV		27
G. Faubert, et. al.	1998	O ₂ Reduction	Fe-Based	LSV	CV on RDE	28
R. Cote, et. al.	1998	O ₂ Reduction	V, Cr, Fe, Co-based		CV on RDE	29
T. Schmidt, et. al.	1998	Hydrogen	Pt/C	CV	LVS on RDE	30
S. Gojkovic, et. al.	1999	O ₂ Reduction	FeTMPP-Cl/BP		CV, LVS on RDE	31
A. Pozio, et. al.	2000	Hydrogen	PtRu/C, PtMo/C	LSV, EI		32
R. Monaharan, et. al.	2001	Methanol	Pt, PtRu, Pd	CV		33
U. Paulus, et. al.	2001	O ₂ Reduction	Pt/C		LVS on RDE	34
D. Chu, R. Jiang	2002	Methanol	PtRu	CV, LSV		35
S-J. Shin, et. al.	2002	Hydrogen	Pt/C	CV, EI		36
C. Rice, et. al.	2003	Formic Acid	Pt, PtRu, PtPd	CV, LSV, CA		37
J. Solla-Gullon, et. al.	2003	Hydrazine	PtPd/Au	CV		38
E. Gyenge	2004	Borohydride	Au, Pt wires	CV, CA, CP, EI		39
D-J Guo, H-L Li	2004	Hydrazine	Pd/Carbon Nanotube	CV, CA		40
J. Lovic, et. al.	2005	Formic Acid	Pt/C	CV, CA		41
M. Atwan, et. al.	2005	Borohydride	Os-alloys	CV,CP, CA		42
R. Olivera, et. al.	2006	Ethanol	RhPt/Pt	CV, LSV, CA		43
X. Li, I-M Hsing	2006	Formic Acid	PtOd	CV, LSV, CA		44

CA- Chronoamperometry, CC- Chronocoulometry, CP- Chronopotentiometry, CV- Cyclic Voltammetry, EI- Electrochemical Impedance, LSV- Linear Sweep Voltametry
FeTMPP-Cl/BP- Organometallic Compound

the GC electrode surface yielding for each of the investigated catalysts a constant load per metal basis of 141 mg cm². The dispersed catalyst on the GC substrate was dried in a mild N₂ stream for about 1 h creating good bonding and electronic contact between the supported catalyst and the GC electrode.

A conventional three-electrode cell was used to perform the electrochemical tests. The cell was composed of the dispersed colloidal metal GC, two graphite rods with an area of ~ 10 cm² acting as the

counter-electrode and a Hg/HgO, 2M NaOH (B20B400, Radiometer Analytical S. A.) electrode as the reference electrode with a - 0.068 V potential vs. Ag/AgCl, KCl_{std} (thus will be referred to as the MOE). Cyclic voltammetry, chronoamperometry and chronopotentiometry experiments were carried out in N₂ purged electrolytes at 295 K employing either a PAR 263A or a PARSTAT 2263 computer controlled potentiostat (Princeton Applied Research Inc.) and the associated Power Sweep and Power Step software (part of the

Power Suite package). Voltammetry on a rotating disc electrode (RDE) experiments were performed by using Volta Lab 80 (PGZ402, Radiometer Analytical S. A.) in conjunction with the glassy carbon electrode tip (A35T090, Radiometer Analytical S. A.), RDE (EDI101, Radiometer Analytical S. A.), and speed control unit (CTV101, Radiometer Analytical S. A.). For NaBH_4 oxidation, 2 M NaOH was used with NaBH_4 (Alfa Aesar Inc., purity +97 %wt) concentrations between 0.03 and 1 M.

2.3. Fuel Cell and MEA preparation

Tests on direct borohydride fuel cells were performed using a Lynntech FCTS MTK system in conjunction with FCPower control software and 5 cm² geometric area single fuel cell kits. Membrane electrode assemblies (MEAs) used in this study were prepared in-house by forming and applying the anode side onto a half-MEA with Nafion® 117 membrane supplied by Electrochem Inc. (EC-MEA-C1), where the cathode side consisted of 4 mg Pt cm⁻² and Toray Carbon paper gas diffusion layer. The anode colloidal catalysts with a metal load of 5 mg cm⁻² were applied on a carbon cloth (ECCC1-060, Electrochem. Inc.). The procedure consisted of the following steps: 5 mg cm⁻² on metal(s) bases of the colloidal catalyst was mixed with 1 mg cm⁻² Nafion® 117 (i.e. corresponding volume of Nafion 5%wt solution) and 0.7 ml ethanol. The mixture was sonicated for 45 minutes. Afterwards, the supported catalyst suspension was applied on the carbon cloth by a technique similar to a decal method, followed by drying in a N₂ atmosphere for 12 h. The final stage in the MEA preparation was the hot pressing of the anode catalyst on the carbon cloth substrate, together with another carbon cloth acting as the anodic backing layer onto the Nafion® 117 membrane. Hot pressing was performed at 1200 lb for 2 min at 160°C.

After the hot pressed full MEA was assembled together with the end plates in the fuel cell test station, membrane conditioning was performed by recirculating a solution of 2 M NaOH at 60 ml min⁻¹ for 2 h prior to each test. The pure sodium hydroxide solution was then replaced by a 2 M NaBH_4 in 2 M NaOH solution at feed rates of 20, 50, and 85 ml min⁻¹. The oxygen flow rate was fixed at 0.2 l min⁻¹ for all tests, with a gauge pressure of 25 psi. The tests were started after the fuel cell temperature and the fuel feed flow stream temperatures reached either 298 K or 333 K. Potential vs. current data were recorded.

3. RESULTS AND DISCUSSION

3.1. Voltammetry of Borohydride Oxidation on Static Electrodes

Figure 1 shows the linear voltammograms obtained on a static electrode. The last peak potentials represent the direct borohydride oxidation peaks. As shown in Table 1, the most negative peak potential was recorded on Pt-Ir, followed by Pt-Ni, Pt-Au, Pt, Au-Pd and Au, respectively.

3.2. Voltammetry of Borohydride Oxidation on Dynamic Electrodes (RDE)

Fig. 2 shows the linear voltammograms obtained on dynamic electrodes (RDE). As for the static electrodes, and as shown in Table 2, the most negative peak potentials were recorded on Pt-Ir, followed by Pt-Ni, Pt, Pt-Au, Au-Pd, and Au, respectively. As illus-

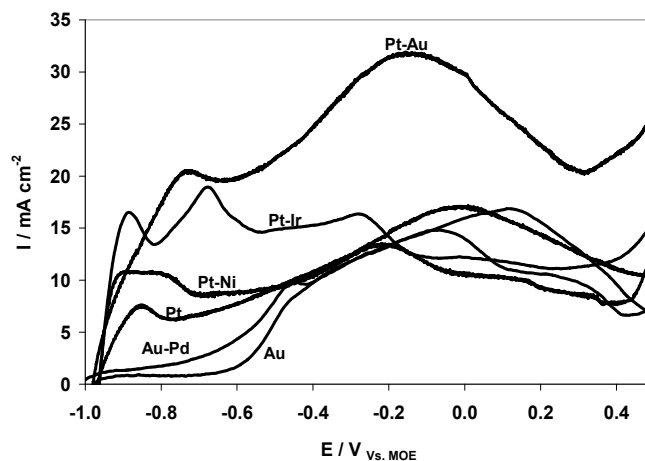


Figure 1. Linear voltammograms of BH_4^- oxidation on colloidal catalysts using a static electrode showing the effect of BH_4^- concentration. Scan rate 100 mV s⁻¹, 298 K. NaBH_4 concentration 0.1 M in 2 M NaOH [50, 51].

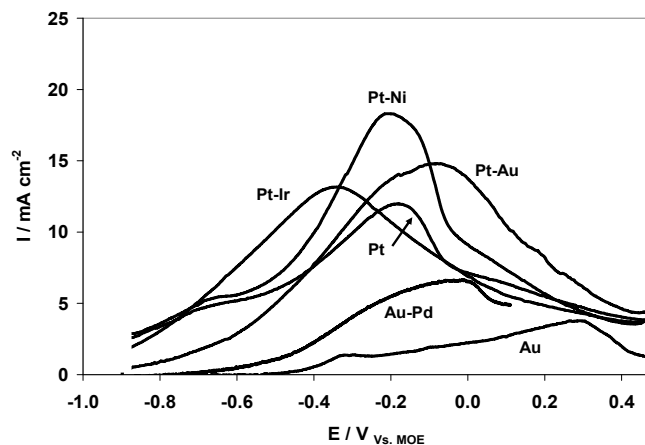


Figure 2. Linear voltammetry of BH_4^- oxidation on colloidal catalysts using a rotating electrode. Scan rate 5 mV s⁻¹, 298 K. NaBH_4 concentration 0.3 M in 2 M NaOH. 500 rpm [50, 51].

Table 1. Peak current densities (I_p) and potentials (E_p) determined from CV (at 100 mV s⁻¹ and 0.1 M NaBH_4) data using supported colloidal catalysts with Nafion 117 polymer electrolyte.

Catalysts	E_p (V)	I_p (mA cm ⁻²)
Pt	-0.014	16.97
Pt-Au	-0.14	31.67
Pt-Ni	-0.206	13.36
Pt-Ir	-0.266	16.28
Au	0.125	16.9
Au-Pd	-0.07	14.8

trated in Fig. 3 [52], plots of $\log i$ vs. η ($\eta = E - E_{OC}$) were made using the data from the exponential increase domain of Fig. 2, and the Tafel equation (eq. 1) was used to calculate the apparent Tafel

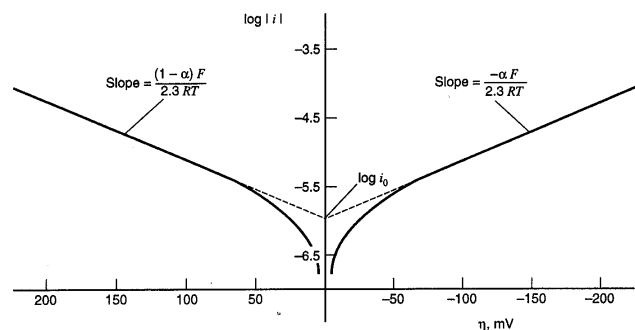


Figure 3. Experimental determination of exchange current density i_o and Tafel slope b [52].

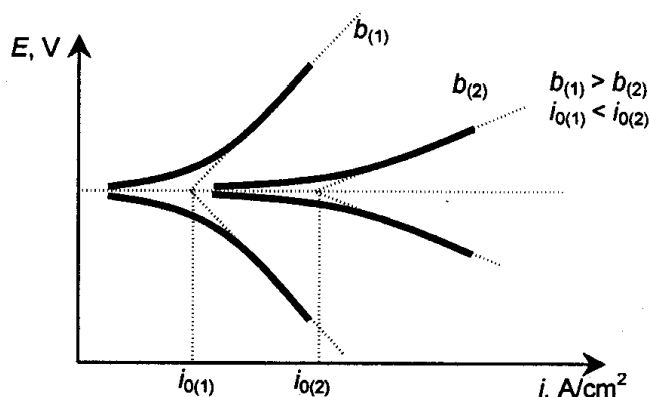


Figure 4. Schematic representation showing the effect of the Tafel slope, b , on the exchange current density, i_o , and the overpotential, η [9].

Table 2. Apparent Tafel slopes, b_a , and exchange current densities, i_o determined from RDE (at 500 rpm and 0.3 M NaBH₄) data using supported colloidal catalysts with Nafion 117 polymer electrolyte.

Catalysts	E_p (V)	I_p (mA cm ⁻²)	b_a (V dec ⁻¹) 298 K	I_o (A cm ⁻²) 298 K
Pt	-0.175	11.9	0.939	2.64×10^{-3}
Pt-Au	-0.075	14.77	0.662	1.18×10^{-3}
Pt-Ni	-0.197	18.25	0.651	1.50×10^{-3}
Pt-Ir	-0.355	13.09	0.823	3.62×10^{-3}
Au	0.293	3.78	1.121	0.076×10^{-3}
Au-Pd	0.0	6.6	0.938	0.120×10^{-3}

Table 3. Fuel cell performance expressed in mA cm⁻² at 0.5 V, for different Anode supported colloidal catalysts with a Nafion 117 polymer electrolyte at both 298K and 333K.

Catalyst	E_p (V) (RDE)	Overpotential (η , V) at 0.01 A cm ⁻²	Current Density, mA cm ⁻² at Cell Voltage of 0.5 V	
			298K	333K
Pt	-0.175	0.542	34.18	85.50
Pt-Au	-0.075	0.614	26.86	92.79
Pt-Ni	-0.197	0.536	43.95	105
Pt-Ir	-0.355	0.363	46.39	105
Au	0.293	2.380	12.20	29.30
Au-Pd	0.0	1.80	14.70	61

slopes and exchange current densities.

$$\eta = b \log \frac{i}{i_o} \quad (1)$$

where η , is the overpotential, b_a , is the Tafel slope, i , is the operating current density, and i_o , is the exchange current density.

Table 2 summarizes the apparent Tafel slopes and exchange current densities of the investigated electrocatalysts. The apparent Tafel slope values are high, being at least four times higher than the values expected based on pure electrode kinetics (e.g. a b value of 0.18–0.19 V was reported for BH₄⁻ oxidation on Pt [39]). These values are a composite of mass transfer and ohmic limitations inside the catalyst layer through the Nafion® film coupled with intrinsic electrode kinetics [12, 13].

Lower values of the Tafel slope, b_a , for an electrocatalyst indicates a higher catalytic activity towards the fuel electrooxidation, since lower values will lead to lower overpotentials [8, 9]. A higher exchange current density, i_o , on the other hand, will minimize the

term ($\log \frac{i}{i_o}$) for a fixed applied current, and thus lower the overpotential accordingly.

It is obvious from Table 2 that the electrocatalysts with the most negative peak potentials showed higher exchange current densities, and lower Tafel slopes compared to those with more positive peak potentials. The Tafel slope is as important as exchange current density in determining the overpotential at a certain operating current density [8]. Optimum values of b_a , as low as possible, and i_o , as high as possible will lead to lower overpotential values, Fig. 4 [9]. It was also proposed that Tafel slope has more impact on overpotential value than exchange current densities [8]. This is at odds with our data for Pt-Ir and Pt-Ni electrocatalysts. Although Pt-Ni showed a lower Tafel slope compared to Pt-Ir, the overpotential was lower for Pt-Ir than that for Pt-Ni, since Pt-Ir had a higher exchange current density: Tables 2 and 3.

3.3. Fuel Cell Performance

Figures 5 and 6 show the fuel cell performance of the investigated electrocatalysts at 298 K and 333 K, respectively. Pt-Ir and Pt-Ni were the most active and exhibited the best performance. This was because they had the most negative peak potentials and lowest overpotentials amongst the investigated electrocatalysts. This is in a good agreement with the RDE results, where they exhibited the highest exchange current densities.

Table 3 clearly shows that the electrocatalysts with the most negative peak potentials show the best performance at both 298K and 333K. It is also clear from Table 3 that the overpotential calculated at an operating current density, i , of 0.1 A cm⁻² was lowest for the electrocatalyst with the most negative peak potential.

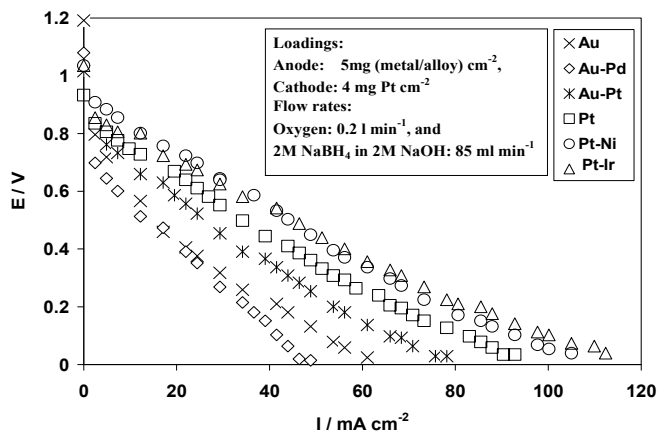


Figure 5. Direct borohydride fuel cell polarization curves at 298 K: Comparison between the colloidal catalysts. Anode catalyst load 5 mg cm⁻². 50 ml min⁻¹ 2 M NaBH₄ – 2 M NaOH. Cathode catalyst (Pt) load 4 mg cm⁻². O₂ flow rate 200 ml min⁻¹ at 2.7 atm [50, 51].

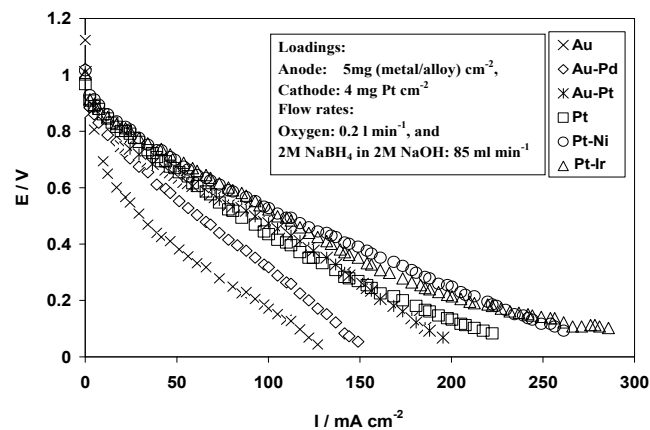


Figure 6. Direct borohydride fuel cell polarization curves at 333 K: Comparison between the colloidal catalysts. Anode catalyst load 5 mg cm⁻². 50 ml min⁻¹ 2 M NaBH₄ – 2 M NaOH. Cathode catalyst (Pt) load 4 mg cm⁻². O₂ flow rate 200 ml min⁻¹ at 2.7 atm [50, 51].

4. CONCLUSIONS

The relationship between both the static and the dynamic CV results and the fuel cell station tests has been investigated for the range of colloidal electrocatalysts. It was found from both static and dynamic CV and the fuel cell station tests that the most active catalyst is the one that shows the most negative oxidation peak potential. Therefore, CV and RDE tests are the electrochemical techniques to use for a reliable assessment of electrocatalysts prior to performing a “real” fuel cell test.

5. ACKNOWLEDGEMENTS

The authors would like to thank the Natural Resources and Engineering Research Council of Canada for their financial support of this work. They would also like to thank Dr. Charles Macdonald

(Department of Chemistry and Biochemistry, University of Windsor) for provision of laboratory facilities and assistance with the preparation of the colloidal electrocatalysts.

6. REFERENCES

- [1] J. Wang, Analytical Electrochemistry, Wiley-VCH, New York (2000) 1-27.
- [2] C. Hamann, A. Hamnett, W. Vielstich, Electrochemistry, Wiley-VCH, New York (1998) 217-274.
- [3] B. Rossiter, J. Hamilton, Physical Methods of Chemistry, John Wiley, New York (1998) 1-50.
- [4] A. Brad, M. Mirkin, Scanning Electrochemical Microscopy, Marcel Dekker, New York (2001).
- [5] E. Smotkin, R. Diaz-Morales, Ann. Rev. Mater. Res., 33 (2003) 557-579.
- [6] R. Jiang, D. Chu, J. Elect. Chemistry, 527 (2002) 137-142.
- [7] E. Reddington, A. Sapienza, B. Gurau, R. Viswantha, S. Saranagani, E. Smotkin, T. Mallouk, Science, 280, 12 (1998) 1735-1737.
- [8] E. Gileadi, Electrode Kinetics for Chemists, Chemical Engineers, and Materials Scientists, VCH, NY (1993) 179-183.
- [9] S. H. Jordanov, P. Paunovic, O. Popovski, A. Dimitrov, D. Slavkov, Bull. Chem. Tech. of Macedonia, 23 (2) (2004) 101-112.
- [10] R. Greef, R. Peat, L. Peter, D. Pletcher, J. Robinson, Instrumental Methods in Electrochemistry, John Wiley, New York (1985) 229-250.
- [11] J. Newman, Electrochemical Systems, Prentice Hall, New York (1991) 454-495.
- [12] M. Perry, J. Newman, E. Cairns, J. Electrochem. Soc., 145, 5 (1998).
- [13] J. O'M Bockris, S. Khan, Surface Electrochemistry: A Molecular Approach, Plenum Press, New York (1993) 280-283, 621.
- [14] M. Janssen, J. Moolhuysen, Electrochimica Acta, 21 (1976) 869-878.
- [15] B. McNicol, R. Short, Electroanal. Chem., 81 (1977) 249-260.
- [16] A. Aramata, R. Ohnishi, J. Electroanal., Chem., 162 (1984) 153-162.
- [17] A. Aramata, T. Kodera, M. Masuda, J. Applied Electrochem, 18 (1988) 577-582.
- [18] S. Swathiranjani, Y. Mikhail, J. Electrochem. Soc., 138, 5 (1991) 1321-1326.
- [19] A. Parthasarathy, C. Martin, J. Electrochem. Soc., 138, 4 (1991) 916-921.
- [20] F. Uribe, T. Springer, S. Gottesfeld, J. Electrochem. Soc., 139, 3 (1992) 765-773.
- [21] A. Parthasarathy, S. Srinivasan, A. Appleby, J. Electroanal., Chem., 339 (1992) 101-121.
- [22] S. Mukerjef, S. Srinivasan, J. Appleby, Electrochimica Acta, 38, 12 (1993) 1661-1669.
- [23] L. Burke, J. Casey, J. Morrissey, J. O'Sullivan, J. Applied Electrochem, 24 (1994) 30-37.
- [24] P. Biswas, Y. Nodasaka, M. Enoy, J. Applied Electrochem, 26

- (1996) 30-35.
- [25]P. Kauranen, E. Skou, J. Munk, J. Electroanal., Chem., 404 (1996) 1-13.
- [26]T. Schmidt, M. Noeske, H. Gasteiger, R. Behm, Langmuir, 13, 10 (1997)2591-2595.
- [27]G. Lalande, R. Cote, D. Guay, J. Dodelet, L. Weng, P. Bertrand, Electrochimica Acta, 42, 9 (1997) 1397-1388.
- [28]G. Faubert, R. Cote, D. Guay, J. Dodelet, G. Denes, C. Poleunis, P. Bertrand, Electrochimica Acta, 43, 14-15 (1998) 1969-1984.
- [29]R. Cote, G. Lalande, G. Faubert, D. Guay, J. Dodelet, G. Denes, J. New Mat. Electrochemical Systems 1, 7 (1998) 7-16.
- [30]T. Schmidt, H. Gasteiger, G. Stab, P. Urban, D. Kolb, R. Behm, J. Electrochem. Soc., 145, 7 (1998) 2354-2358.
- [31]S. Gojkovic, S. Gupta, R. Savinell, Electrochimica Acta, 45 (1999) 889-897.
- [32]A. Pozio, L. Giorgi, E. Antolini, E. Passalacqua, Electrochimica Acta, 46 (2000) 555-561.
- [33]R. Monaharan, J. Prabhuram, J. Power Sources, 96 (2001) 220-225.
- [34]U. Paulus, T. Schmidt, H. Gasteiger, R. Behm, J. Electroanal. Chem., 495 (2001) 134-145.
- [35]D. Chu, R. Jiang, Solid State Ionics, 148 (2002) 591-599.
- [36]S-J. Shin, J-K., Lee, H-Y. Ha, S-A., Hong, H-S. Chun, I-H., Oh, J. Power Sources, 106 (2002) 146-152.
- [37]C. Rice, S. Ha, R.I. Masel, A. Wieckowski, Journal of Power Sources, 115 (2003) 229-235.
- [38]J. Solla-Gullón, A. Rodes, V. Montiel, A. Aldaz and J. Clavilier, J. Electroanalytical Chemistry, 554-555 (15) (2003) 273-284.
- [39]E. Gyenge, Electrochim. Acta 49 (2004) 965 and 49 (2004)1875.
- [40]Dao-Jun Guo, Hu-lin Li, Electrochemistry Communications, 6 (2004) 999-1003.
- [41]J.D. Lovic', A.V. Tripkovic', S.Lj. Gojkovic', K.Dj. Popovic', D.V. Tripkovic', P. Olszewski, A. Kowal, Journal of Electroanalytical Chemistry, 581 (2005) 294-302.
- [42]Mohammed H. Atwan, Derek O. Northwood, Elod L. Gyenge, Int. J. Hydrogen Energy, 30 (12) (2005)1323-1331.
- [43]R.T.S. Oliveira, M.C. Santos, B.G. Marcussi, S.T. Tanimoto, L.O.S. Bulhoes, E.C. Pereira, Journal of Power Sources, 157 (2006) 212-216.
- [44]Xuguang Li, I.-Ming Hsing, Electrochimica Acta, 51 (2006) 3477-3483
- [45]H. Bönnerman, W. Brijoux, R. Brinkmann, E. Dinjus, T. Joußen, B. Korall, Angew. Chem. Int. Engl., 1991; 30(10):1312-1314.
- [46]M. Götz and H. Wendt, Electrochim Acta 1998; 43(24):3637-3644.
- [47]R. Richards, R. Mortel, H. Bonnemann, Fuel Cell Bulletin, 2001; 4(37):7-10.
- [48]H. Bönnerman, private communication, October 16, 2003.
- [49]H. Bönnerman, U. Endruschat, J. Hormes, G. Kohl, S. Kruse, H. Modrow, R. Mortel, K.S. Nagabhushana, Fuel Cells, 2004; 4(3):297-308.
- [50]Elöd Gyenge, M. Atwan, Derek Northwood, J. Electrochem. Soc., 153 (1) (2006) A150-A158.
- [51]Mohammed H. Atwan , Charles L.B. Macdonald b, Derek O. Northwood, Elod L. Gyenge, J. Power Sources, 158 (2006) 36-44.
- [52]A. J. Bard, L. R. Faulkner, Electrochemical Methods, Fundamentals and Applications, 2nd Ed., JW, NY (2001) 156-260, 331-348.

